DIFFERENTIAL ANALYSIS OF GENOME-WIDE METHYLATION AND GENE EXPRESSION IN MESENCHYMAL STEM CELLS OF PATIENTS WITH FRACTURES AND OSTEOARTHRITIS

Alvaro del Real[1]*, Flor M. Pérez-Campo [1,2]*, Agustín F. Fernández[3], Carolina Sañudo[1], Carmen G. Ibarbia[1], María I. Pérez-Núñez[4], Wim Van Criekinge[5], Maarten Braspenning[6], María A. Alonso[4], Mario F. Fraga[3] and Jose A. Riancho[1]

* Alvaro del Real and Flor M. Pérez-Campo contributed equally to this study.

[1] Department of Medicine and Psychiatry, University of Cantabria, and Service of Internal Medicine, Hospital U.M. Valdecilla-IDIVAL, Santander, Spain.

[2] Present address: Department of Molecular Biology. University of Cantabria, Santander, Spain.

[3] Cancer Epigenetics Laboratory, Institute of Oncology of Asturias (IUOPA), HUCA, University of Oviedo, Oviedo. Spain.

[4] Service of Traumatology and Orthopedic Surgery, Hospital U.M. Valdecilla, University of Cantabria, Santander, Spain.

[5] Mathematical Modelling, Statistics and Bio-informatics, Faculty Bioscience Engineering, University Ghent, Coupure Links 653, 9000 Gent, Belgium.

[6] NXT-Dx, Fr. Rooseveltlaan 349/B.43, 9000 Gent, Belgium.

ADDRESS CORRESPONDENCE TO:

José A. Riancho, Department of Medicine and Psychiatry, University of Cantabria. Av Valdecilla sn. 39008 Santander, Spain
Tel +3442201990
Fax +34942201695
Email: rianchoj@unican.es

ABSTRACT

Insufficient activity of the bone-forming osteoblasts leads to low bone mass and predisposes to fragility fractures. The functional capacity of mesenchymal stem cells (hMSCs), the precursors of osteoblasts, may be compromised in elderly individuals, in relation with the epigenetic changes associated with aging. However, the role of hMSCs in the pathogenesis of osteoporosis is still unclear. Therefore we aimed to characterize the genome-wide methylation and gene expression signatures and the differentiation capacity of hMSCs from patients with hip fractures. We obtained hMSCs from the femoral heads of women undergoing hip replacement due to hip fractures and controls with hip osteoarthritis. DNA methylation was explored with the Infinium 450K bead array. Transcriptome analysis was done by RNA sequencing. The genomic analyses revealed that most differentially methylated loci were situated in genomic regions with enhancer activity, distant from gene bodies and promoters. These regions were associated with differentially-expressed genes enriched in pathways related to hMSC growth and osteoblast differentiation. hMSCs from patients with fractures showed enhanced proliferation and up-regulation of the osteogenic drivers RUNX2/OSX. Also, they showed some signs of accelerated methylation aging. When cultured in osteogenic medium, hMSCs from patients with fractures showed an impaired differentiation capacity, with reduced alkaline phosphatase and poor accumulation of a mineralized matrix. Our results point to two areas of potential interest for discovering new therapeutic targets for low bone mass disorders and bone regeneration: the mechanisms stimulating MSCs proliferation after fracture and those impairing their terminal differentiation.

RUNNING TITLE: Transcriptome and Methylome Analysis of MSCs in Fractures and Osteoarthritis.

KEYWORDS: Osteoporosis, Osteoarthritis, Epigenetics, Stem cells, Transcription factors.

INTRODUCTION

Osteoporotic hip fractures have a particularly negative impact on the patients' quality of life and life expectancy. The pathogenetic mechanisms of osteoporosis are not completely understood, but they imply an imbalance in bone remodelling, with a predominance of bone resorption over bone formation. Osteoblasts are the cells responsible for bone formation. Human mesenchymal stem cells (hMSCs) are pluripotent cells capable of differentiating into osteoblasts, chondrocytes, adipocytes and myoblasts. Therefore, hMSCs are the subject of considerable interest from a double perspective. On the one hand, hMSC malfunction may be involved in the pathogenesis of osteoporosis [1,2]. Thus, elucidating the mechanisms involved in hMSCs proliferation and differentiation could point to new drug targets to improve osteoblast function in osteoporotic patients. On the other hand, the infusion of hMSCs could theoretically improve bone formation systemically or locally. A few studies tried to characterize hMSCs from patients with osteoporosis, but the results are controversial [3–5]. Therefore, much more basic research is needed to characterize hMSCs in osteoporosis prior to use them for the treatment of skeletal disorders.

Epigenetic mechanisms play an important role in skeletal biology. In particular, DNA methylation has been shown to modulate the differentiation of cells towards the osteoblastic lineage [6,7]. Thus, it is tempting to speculate that changes in DNA methylation influence the differentiation capability of hMSCs in osteoporosis. However there are only scarce data about the methylation signature of skeletal hMSCs. Therefore, we aimed to perform a genome-wide methylome analysis of hMSCs from patients with hip fractures and explore the functional consequences at the transcriptome level and the ability to proliferate and differentiate *in vitro*.

RESULTS

Isolation and characterization of hMSCs

We had similar success rate in establishing an hMSC culture with samples obtained from patients with fractures (27 out of 41, 66%) or with OA (22 out of 32, 69%). The hMSC phenotype was confirmed by flow cytometry using a combination of markers ($CD45^-$, $CD34^-$, $CD90^+$, $CD73^+$, $CD105^+$) that define the phenotype of bone marrow hMSCs [2] (Supplemental Fig. *S1*).

DNA methylation profiling

When the interrogated CpGs were grouped according to their genomic position, gene bodies were more methylated than CG islands or gene promoters (Supplemental Figs. *S2* and *S3*). The average methylation level was similar in both study groups. Nevertheless, among the 477708 sites explored, we found 9038 differentially methylated CpG sites. Of them, 4417 were more methylated and 4621 were less methylated in samples obtained from osteoporotic patients with hip fracture (FRX)**.** Among the differentially methylated CpG sites, 1586 sites were located in CpG islands, 1105 in shores, 353 in shelves and 5994 sites in open sea.

The analysis at the region level revealed 217 out of 30877 gene promoters with differential methylation, which correspond to 71 protein coding genes, of a total of 21191 different genes, including 111 more methylated and 106 less methylated in FRX**.** Regarding gene bodies, 62 were found more methylated and 67 less methylated in FRX. Among CG islands, 16 were more methylated and 24 less methylated in FRX (Table 1 and Supplemental Fig. *S4*).

Differential methylated sites were enriched in enhancers regions (which included 2425 of the 9038 differentially methylated CpGs). The distances to the transcription start sites (TSSs) are shown in Supplemental Figure *S5*. The region level analysis revealed 1684 differential methylated gene enhancer regions; 870 regions (associated with 722 protein-coding genes) were hypermethylated and 814 (678 genes) were hypomethylated in FRX in comparison with OA (Supplemental Table *S1* and Figure *1A*). Most FRX and OA samples tended to be grouped in common clusters, but there was some degree of overlapping, as shown in Fig. *1B*. Genes with differentially-methylated enhancers were overrepresented among pathways related to stem cell development and bone-related pathways, like the Wnt receptor signaling pathway (p=4.5x10^{-8} binomial test), regulation of osteoblast differentiation (p=9.1x10^{-5}), regulation of hMSCs proliferation (p=7.6x10^{-6}) and bone mineralization (p=7.6x10^{-4}) pathways (Supplemental Fig. *S6*).

Gene expression analysis

Overall, 11390 genes were expressed in both FRX and OA samples, whereas 496 genes were expressed only in FRX and 1695 in OA. As expected, the gene expression signature was typical of hMSCs (Supplemental Table *S2*)**.** Overall, 99 protein-coding genes were up-regulated in FRX (FDR<0.10 and fold-change>2), whereas 239 were down-regulated (Supplemental Fig. *S7* and Supplemental Table *S3*). The top 50 up- or down-regulated genes are shown in Tables 2 and 3.

Among genes with differential expression, those up-regulated in FRX were enriched in pathways related to hMSCs differentiation and bone formation, whereas those down-regulated in FRX were enriched in pathways related to the immune response, among others **(**Supplemental Table *S4***).**

Correlation between differential DNA methylation and differential gene expression

Genes with differentially methylated enhancers were overrepresented among those showing differential expression (19.8% versus 9.2% in those without differential expression; p=1.2x10^{-10}). The direction of the association was variable, but there was a trend for an inverse correlation between enhancer methylation and expression (Odds Ratio [OR] 0.3; 95% confidence interval 0.12-0.99; p=0.05). This is schematically depicted in *Fig. 2A*, showing that 18 genes up-regulated in FRX had differentially methylated enhancers, 8 hypermethylated and 10 hypomethylated. On the other hand, 55 genes down-regulated in FRX had differentially methylated enhancers; 39 hypermethylated and 16 hypomethylated. Examples of the individual values of expression and methylation of some genes are shown in Supplemental Fig. *S8*. The comparative Gene Ontology Enrichment analysis revealed that genes with hypomethylated enhancers and up-regulated expression in fractures were overrepresented in pathways related to hMSCs proliferation, osteoblast differentiation and bone mineralization, as well as some neuron-related pathways **(**Figure *2B* and Supplemental Figure *S9*).

Validation of expression and methylation differences across groups

We confirmed, by qPCR, the expression pattern of 10 genes among those that showed differential expression in the RNAseq analysis (*SPARC, LOXL2, FOXP2, LAMC1, SLC5A3, OPG, ID2, LASP1, IGFBP4* and *UNC5B*), including 8 samples previously analysed by RNAseq and 19 new samples. There were strong correlations in the individual results obtained with both techniques (Supplemental Figs *S10* and *S11*). Similarly, to validate the results obtained with the 450k array, we analysed by pyrosequencing four genes showing differential methylation according to array data analysis (Supplemental Figure *S12*).

DNA methylation age

We studied the DNA methylation aging in our samples by using a software based on Illumina DNA Infinium 450K data that analyses a set of genes showing age-related changes in methylation. There was a significant correlation between the epigenetic age and the chronological age (r=0.64, p=1.357e-05). The slopes of the regression lines were similar in both patient groups (Figure *3, left panel*), but the lines were vertically displaced. Therefore, when the regression was computed with both groups combined, the deviations of the epigenetic age from the chronological age were higher in the FRX group than in the OA group, thus suggesting accelerated epigenetic aging in the former (Fig. *3, right panel*).

Proliferative capability of hMSCs

Interestingly, the proportion of actively-dividing, Ki-67 positive cells was significantly higher among hMSCs grown from patients with FRX (Figure *4A*). These results agreed with those obtained from a MTT assay, which confirmed a higher proliferation rate in hMSCs cultures established from patients with fractures (Figure *4B*).

Transcriptional signature and bone differentiation capacity of hMSCs

Analysis of the gene expression levels of a set of osteogenic and adipogenic markers showed significant differences in the expression levels of key osteogenic genes (Figure *4C*), such as *OSX, ALPL, SPP1* and *BGLAP,* between patients with osteoporotic fractures and OA. These data agreed and validated the previously shown results from the RNAseq analysis. Interestingly, *OSX*, a key transcription factor expressed in the first stages of osteoblast development was significantly up-regulated in hMSCs from patients with FRX whereas collagen expression was similar in both groups. Markers, such as *ALPL* and *SPP1*, normally expressed later on during the osteogenic differentiation process, were down-regulated in hMSCs isolated from patients with osteoporotic fractures. On the

other hand, adipogenic markers, such as *PPARG* and *LPL*, were expressed less abundantly in patients with fractures than in those with OA (Fig. *4C*).

In line with their hMSC phenotype, the cells were able to differentiate normally into adipocytes and osteoblasts (Fig. *5A*). However, there were marked differences between groups and the capacity to form a mineralized matrix was markedly diminished in hMSCs from patients with FRX (p=0.00015; Fig. *5B*). The alkaline phosphatase activity in hMSC cultures from FRX was also much lower than in cultures of OA origin (Fig. *5C*), and there was a correlation between alkaline phosphatase activity and matrix mineralization (Spearman's rho 0.84, $p<0.001$). On the other hand, there was a tendency for enhanced *OSX* and *RUNX2* expression in FRX cells (Fig. 5*D*)**.**

DISCUSSION

We have previously shown that modifications in DNA methylation play a central role in the differentiation of cells along the osteoblastic lineage and that genes related to skeletal development are differentially methylated in bone samples of patients with osteoporotic fractures [8]. In the present study, we explored the epigenome of hMSCs in patients with fractures. To our knowledge, this is the first study combining epigenome-wide and transcriptome-wide analyses of hMSCs in osteoporosis. We established that the methylation signatures of hMSCs from patients with fractures and OA show significant differences at the enhancer regions of a number of genes related to cell proliferation and differentiation.

Our study has some limitations. The method used does not allow distinguishing methylated and hydoxymethylated cytosines. Due to practical reasons, we isolated hMSCs from the bone marrow of OA patients rather than normal bone marrow as comparison controls. Nevertheless, it has been suggested that MSCs from OA patients have similar proliferation and osteogenic differentiation

capacity to MSCs from healthy donors [9]. Also, we removed the subchondral region, thus trying to avoid the potential influence of the changes taking place in the subchondral bone [10]. Aging is associated with methylation differences in some genes [11] and patients with fractures were somewhat older than those with OA. Nevertheless, we adjusted the results including age as a covariate to avoid any age-related bias. Also, due to the low percentage of hMSCs in bone marrow (less than 1/10,000 to 1/100,000) hMSCs needed to be expanded in vitro prior to the analysis. However, to avoid changes in the epigenome signature that could bias the results, in vitro expansion was kept to a minimum and only cells at first passage were used for the analyses.

The classical view of DNA methylation tended to associate increased methylation with decreased gene expression and vice versa. However, our results confirm that the relationship between methylation and expression is indeed variable. Although increased methylation was associated with a decreased expression of many genes, the opposite was also true. In fact, that seems to be the case in other cell types [12,13]. Additionally, as previously reported in other conditions, including the osteoarthritic cartilage [14,15], most differentially methylated regions do not appear to be at the gene bodies or at promoter regions, but at genomic regions with enhancer activity distant from the promoter. Thus, changes in methylation at regulatory regions may influence the expression of genes situated several hundred kilobases away. Also, as shown in our genomic region analysis, most regions showing differential methylation between groups appear to be outside CpG islands.

Rather unexpectedly, hMSCs from patients with hip fractures tended to display up-regulation of genes linked to cell proliferation pathways, in parallel with a decreased methylation of their enhancer regions. Those genes were over-represented in important pathways, such as those regulating cell proliferation, osteoblast differentiation or vasculogenesis. This translated into an increased proliferation of these cells, in comparison with cells from patients with OA, in line with the concept

that fractures activate and mobilize hMSCs and are consistent with previous reports showing a mobilization of MSCs into the circulation in response to fracture [16]. The mechanisms involved remain to be elucidated, but may include the release of activating cytokines and activation of the Wnt pathway, as suggested by our enrichment analysis. Wnt ligands promote the proliferation of osteoblasts precursors [17,18]. In line with this, Baht et *al*. recently reported that hematopoietic cells of young mice are able to stimulate the osteoblastic responses in aged animals by a mechanism that involves β-catenin, a critical signaling mediator of the canonical Wnt pathway [19]. Neural-mediated mechanisms may also be included, as suggested by the enhanced bone formation shown by patients with head trauma [20] and the differential methylation and expression of some genes in nervous tissue-related pathways also found in the present study.

MSCs from fracture patients showed an up-regulation of the genes driving osteogenic differentiation, such as *RUNX2* and *OSX*. The expression of some genes such as *BGLAP* and *IBSP*, usually considered as characteristic of the osteoblastic phenotype and targets of RUNX2, was also increased in hMSCs from fracture patients in basal conditions. However, those hMSCs showed a reduced ability to from a mineralized matrix when cultured in osteogenic medium. This could be related to a decreased activity of alkaline phosphatase, which plays a critical role in mineralization, or to the persistent up-regulation of *RUNX2*. RUNX2 is a master driver of osteoblast precursor differentiation [21]. Specific epigenetic marks contribute to the regulation of *RUNX2* expression [22]. RUNX2 controls bone development and osteoblast differentiation by regulating the expression of a significant number of bone-related target genes, including collagen, osteocalcin, osteopontin, bone sialoprotein and osteoprotegerin. Thus, it plays a critical role in the early stages of differentiation of hMSCs into pre-osteoblasts. However, after this initial step, *RUNX2* expression must be turned down to allow terminal differentiation of osteoblasts [23].

Recent experiments in rodent models of osteoporosis have shown that the MSC transplantation may have a positive effect on bone mass locally and even systemically [24,25]. Additionally, molecules helping to target deliver MSCs into bone are being developed [26]. This raises the possibility of using MSCs for bone regeneration, fracture consolidation or treating widespread bone loss. Since allogenic transplants of MSCs pose difficulties related to histocompatibility, in clinical practice autologous transplants would be preferable. In this line, our results are encouraging because they show that, despite some accelerated epigenetic aging, hMSCs from patients with fragility fractures are activated and maintain a good proliferation capacity, rendering them potentially useful for autologous transplants. Indeed, these cells were able to express genes encoding several proteins present in bone matrix in quantities similar to those expressed by cells from OA patients, which have been reported to behave similarly to MSCs from healthy subjects [9]. However, their ability for terminal differentiation and the formation of a mineralized matrix appear to be compromised, at least *in vitro*. Hence, it would be highly desirable to reach a better understanding of the mechanisms impairing that ability in order to circumvent them with the final objective of optimizing bone matrix formation *in vivo*.

In summary, the epigenome-wide signature of hMSCs from fracture patients shows differentially methylated regions in comparison with hMSCs derived from OA patients. Most differences are in genomic regions with enhancer activity, distant from gene bodies and apart from CpG islands. They are associated with up-regulation of a number of genes involved in MSC proliferation and differentiation, including an up-regulation of genes such as *RUNX2/OSX* driving the differentiation towards an osteoblastic phenotype. However, their ability to form a mineralized matrix appears to be impaired. These results point to two areas of potential interest for discovering new therapeutic targets for low bone mass disorders and bone regeneration: the mechanisms stimulating MSCs after fracture and the mechanisms impairing the terminal differentiation of MSCs. Additionally, these results

emphasize the concept that modifications of DNA methylation may have a cis-influence on rather distant genes.

MATERIALS AND METHODS

Human Mesenchymal Stem Cells (hMSCs) isolation and culture

Bone marrow hMSCs were obtained from the femoral heads of patients undergoing replacement surgery due to osteoporotic hip fractures (FRX; *n*=25, age 62 to 88 yrs) or hip osteoarthritis (OA; *n*=17, age: 72 to 92 yrs). They included female patients with osteoporotic hip fractures or hip osteoarthritis. Patients with high-impact fractures, secondary osteoporosis or secondary OA were excluded. All patients gave informed written consent. The study protocol was approved by the institutional review board (Comité de Etica en Investigación Clínica de Cantabria). Cylinders of trabecular bone were extracted with a trephine, after removing the subchondral and subfracture edges, they were washed with 50 mL of phosphate-buffered saline (PBS). Cells were subjected to a density Ficoll gradient. Then, 2 x10^6 per cm^2 were cultured on polystyrene culture flasks in Mesencult^{TM} MSC Basal media completed with 10% of Mesenchymal Stem Cell Stimulatory supplements (Stem Cell Technologies®, Vancouver, Canada). Representative samples were characterized by staining for surface markers in a FACSCanto II flow cytometer (Becton Dickinson, New Jersey, USA) after labelling with antibodies against CD45, CD34, CD73, CD90 and CD105.

Genome-wide methylation analysis

Since only MSCs at first passages were used for the experiments, there had a limited number of cells to perform all experiments with some of the hMSC lines. Thus, only 22 FRX and 17 OA samples of all the samples initially harvested were used for the analyses of DNA methylation (patients age: 62 to 95

yrs). DNA was extracted with Phenol:Chloroform:Isoamyl Alcohol and bisulfite-converted prior to genome-wide analysis of methylation with the Infinium Human Methylation450 BeadChip array (Illumina®, San Diego, CA, USA) in the Spanish "Centro Nacional de Genotipado" (CEGEN-ISCIII).

Raw data files were pre-processed using R/Bioconductor package RnBeads, [27] and methylation was described as β value, which ranges between 0 (no methylation) to 1 (full methylation).Analyses were conducted at the single CpG site level and at various region levels, including age as a covariate. Regions with FDR<0.05 and an absolute difference in methylation higher than 10% ($\Delta\beta$>0.10) were considered as differentially methylated. Annotation data for the genomic enhancers' study were retrieved from the H1 embryonic stem cell line from the UCSC Table Browser.

The methylation level of selected CpGs was replicated by pyrosequencing (PyromarkQ24 Advanced System®). Primers used for PCR amplification and sequencing were designed with the PyroMark assay designer (Supplemental Table S5). The statistical significance of the differences between FRX and OA patients was tested by Mann-Whitney tests, with a significance threshold of 0.05.

Transcriptome analysis

RNA was isolated from hMSCs (*n*=10 FRX and *n*=10 OA) using Trizol® (Thermofisher Scientific, Waltham, MA, USA). After quality check and quantitation, the samples were prepared using the NEBNext Ultra Directional RNA Library Protocol. Samples were sequenced on an Illumina Hi-seq 2000 sequencer (NTX-Dx, Gent, Belgium). Sample reads were mapped to the human reference genome build GRCh37. Expression analysis was done with cufflinks v2.1.1 on Gencode Annotation v15. FPKM values were calculated for each annotated gene and transcript. RNAseq analysis was carried out at the transcript level with Altanalyze software [28] and at the gene level with the

Bioconductor package EdgeR [29]. Genes with FDR<0.10 and fold-changes >2 were regarded as differentially expressed.

Enrichment analyses of the genes with differentially-methylated enhancers were obtained from the output of GREAT software [30]. The overrepresentation of genes with differential expression in different cell pathways (Wikipathways) was obtained from the output of WEBGESTALT software [31], which incorporates information from different public resources. The Gene Ontology enrichment analyses from the common terms between differentially-methylated enhancers and differential expression were done with ArrayTrack software [32].

RNAseq data and expression of selected genes were confirmed by using real-time quantitative PCR (qPCR), after reverse-transcription of RNA into cDNA, using the housekeeping genes *GAPDH* and *RPL13A* for normalization. Assay details are given in **Supplemental Table S5**.

DNA methylation age

The epigenetic age was calculated from the methylation level of a set of 353 CpGs which has been shown to change with aging in a wide variety of tissues [33]. The relationship of the epigenetic age and the chronological age was explored by linear regression analysis.

Proliferation Analysis

The proliferation status of hMSCs was assessed by immunocytochemistry using an anti-Ki-67 antibody, a nuclear protein associated with cell proliferation. The results were confirmed by a cell proliferation colorimetric assay based on the reduction of the tetrazolium dye MTT.

Osteogenic and Adipogenic Differentiation

hMSCs were cultured in osteogenic induction medium (low glucose Dulbecco Modified Eagle Medium (DMEM) with 10% FBS, 50 μM ascorbic acid, 10 mM β-glycerophosphate, 100 nM dexamethasone) or adipogenic induction medium (DMEM, supplemented with 1.0 M dexamethasone, 0.2 mM indomethacin, 0.5 mM 3-isobutyl-1-methylxanthine, 10% FBS). hMSCs were plated in a 24 wells plate and incubated for up to 3 weeks, prior to staining or RNA extraction. The formation of mineralized matrix was assessed by Alizarin Red staining. The staining was evaluated semiquantitatively by two independent observers who were blind of the culture origin. Other wells were used to determine alkaline phosphatase activity in cell lysates by a colorimetric method based on the ability of ALPL to hydrolyze p-nitrophenylphosphate, [34]. Oil Red was used to visualize the presence of lipid droplets.

AUTHORSHIP AND ACKNOWLEDGMENT

We thank the skillful technical assistance of Jana Arozamena. This study was supported by a grant from Instituto de Salud Carlos III (PI12/615), through a program potentially co-funded by FEDER Funds from the European Union. Carolina Sañudo was partially supported by IDIVAL. The methylation analysis service was carried out at CEGEN-PRB2-ISCIII; it is supported by grant PT13/0001, ISCIII-SGEFI / FEDER

Authors´roles: Study design: JAR, FMPC; Clinical data Collection: CGI, MIPN, MAA; Experimental data collection: FMPC, AR, CS, WVC, MB, AFF; Data analysis and interpretation: WVC, MB, AR, FMPC, MFF, JAR; Drafting Manuscript: AR, FMPC, JAR; Revising Manuscript Content: AR, FMPC, JAR; Approving final version of manuscript: All authors. JAR takes responsibility for the integrity of the data analysis.

DISCLOSURE OF CONFLICTS OF INTEREST

WVC and MB are employees of NTX, the company that performed RNA sequencing. Other authors do not have conflicts of interest relevant to this paper.

REFERENCES

1. Liu H, Xia X, Li B. Mesenchymal stem cell aging: Mechanisms and influences on skeletal and non-skeletal tissues. Exp Biol Med (Maywood) 2015; 240:1099–106.
2. Donoso O, Pino AM, Seitz G, Osses N, Rodríguez JP. Osteoporosis-associated alteration in the signalling status of BMP-2 in human MSCs under adipogenic conditions. J Cell Biochem 2015; 116:1267–77.
3. Haasters F, Docheva D, Gassner C, Popov C, Böcker W, Mutschler W, Schieker M, Prall WC. Mesenchymal stem cells from osteoporotic patients reveal reduced migration and invasion upon stimulation with BMP-2 or BMP-7. Biochem Biophys Res Commun 2014; 452:118–23.
4. Liu W, Qi M, Konermann A, Zhang L, Jin F, Jin Y. The p53/miR-17/Smurf1 pathway mediates skeletal deformities in an age-related model via inhibiting the function of mesenchymal stem cells. Aging (Albany NY) 2015; 7:205–18.
5. Prall WC, Haasters F, Heggebö J, Polzer H, Schwarz C, Gassner C, Grote S, Anz D, Jäger M, Mutschler W, et al. Mesenchymal stem cells from osteoporotic patients feature impaired signal transduction but sustained osteoinduction in response to BMP-2 stimulation. Biochem Biophys Res Commun 2013; 440:617–22.
6. Delgado-Calle J, Sañudo C, Bolado A, Fernández AF, Arozamena J, Pascual-Carra MA, Rodriguez-Rey JC, Fraga MF, Bonewald L, Riancho JA. DNA methylation contributes to the regulation of sclerostin expression in human osteocytes. J Bone Miner Res 2012; 27:926–37.

7. Perez-Campo F, Riancho J. Epigenetic Mechanisms Regulating Mesenchymal Stem Cell Differentiation. Curr Genomics 2015; 16:368–83.

8. Delgado-Calle J, Fernández AF, Sainz J, Zarrabeitia MT, Sañudo C, García-Renedo R, Pérez-Núñez MI, García-Ibarbia C, Fraga MF, Riancho JA. Genome-wide profiling of bone reveals differentially methylated regions in osteoporosis and osteoarthritis. Arthritis Rheum 2013; 65:197–205.

9. Stiehler M, Rauh J, Bünger C, Jacobi A, Vater C, Schildberg T, Liebers C, Günther K-P, Bretschneider H. In vitro characterization of bone marrow stromal cells from osteoarthritic donors. Stem Cell Res 2016; 16:782–9.

10. Li G, Yin J, Gao J, Cheng TS, Pavlos NJ, Zhang C, Zheng MH. Subchondral bone in osteoarthritis: insight into risk factors and microstructural changes. Arthritis Res Ther 2013; 15:223.

11. Roforth MM, Farr JN, Fujita K, McCready LK, Atkinson EJ, Therneau TM, Cunningham JM, Drake MT, Monroe DG, Khosla S. Global transcriptional profiling using RNA sequencing and DNA methylation patterns in highly enriched mesenchymal cells from young versus elderly women. Bone 2015; 76:49–57.

12. Shakhbazov K, Powell JE, Hemani G, Henders AK, Martin NG, Visscher PM, Montgomery GW, McRae AF. Shared genetic control of expression and methylation in peripheral blood. BMC Genomics 2016; 17:278.

13. van Eijk KR, de Jong S, Boks MPM, Langeveld T, Colas F, Veldink JH, de Kovel CGF, Janson E, Strengman E, Langfelder P, et al. Genetic analysis of DNA methylation and gene expression levels in whole blood of healthy human subjects. BMC Genomics 2012; 13:636.

14. Zhang Y, Fukui N, Yahata M, Katsuragawa Y, Tashiro T, Ikegawa S, Michael Lee MT.

Genome-wide DNA methylation profile implicates potential cartilage regeneration at the late stage of knee osteoarthritis. Osteoarthritis Cartilage 2016; 24:835–43.

15. Jeffries MA, Donica M, Baker L, Stevenson M, Annan AC, Humphrey MB, James JA, Sawalha AH. Genome-wide DNA methylation study identifies significant epigenomic changes in osteoarthritic subchondral bone and similarity to overlying cartilage. Arthritis Rheumatol 2016; 68(6):1403-14

16. Alm JJ, Koivu HMA, Heino TJ, Hentunen TA, Laitinen S, Aro HT. Circulating plastic adherent mesenchymal stem cells in aged hip fracture patients. J Orthop Res 2010; 28:1634–42.

17. Qiang Y-W, Barlogie B, Rudikoff S, Shaughnessy JD. Dkk1-induced inhibition of Wnt signaling in osteoblast differentiation is an underlying mechanism of bone loss in multiple myeloma. Bone 2008; 42:669–80.

18. Maupin KA, Droscha CJ, Williams BO. A Comprehensive Overview of Skeletal Phenotypes Associated with Alterations in Wnt/β-catenin Signaling in Humans and Mice. Bone Res 2013; 1:27–71.

19. Baht GS, Silkstone D, Vi L, Nadesan P, Amani Y, Whetstone H, Wei Q, Alman BA. Exposure to a youthful circulaton rejuvenates bone repair through modulation of β-catenin. Nat Commun 2015; 6:7131.

20. Yang T-Y, Wang T-C, Tsai Y-H, Huang K-C. The effects of an injury to the brain on bone healing and callus formation in young adults with fractures of the femoral shaft. J Bone Joint Surg Br 2012; 94:227–30.

21. Lian JB, Gordon JA, Stein GS. Redefining the activity of a bone-specific transcription factor: novel insights for understanding bone formation. J Bone Miner Res 2013; 28:2060–3.

22. Rojas A, Aguilar R, Henriquez B, Lian JB, Stein JL, Stein GS, van Wijnen AJ, van Zundert B,

Allende ML, Montecino M. Epigenetic Control of the Bone-master Runx2 Gene during Osteoblast-lineage Commitment by the Histone Demethylase JARID1B/KDM5B. J Biol Chem 2015; 290:28329–42.

23. Bruderer M, Richards RG, Alini M, Stoddart MJ. Role and regulation of RUNX2 in osteogenesis. Eur Cell Mater 2014; 28:269–86.

24. Antebi B, Pelled G, Gazit D. Stem cell therapy for osteoporosis. Curr Osteoporos Rep 2014; 12:41–7.

25. Kiernan J, Hu S, Grynpas MD, Davies JE, Stanford WL. Systemic Mesenchymal Stromal Cell Transplantation Prevents Functional Bone Loss in a Mouse Model of Age-Related Osteoporosis. Stem Cells Transl Med 2016; 5:683–93.

26. Yao W, Lane NE. Targeted delivery of mesenchymal stem cells to the bone. Bone 2015; 70:62–5.

27. Assenov Y, Müller F, Lutsik P, Walter J, Lengauer T, Bock C. Comprehensive analysis of DNA methylation data with RnBeads. Nat Methods 2014; 11:1138–40.

28. Emig D, Salomonis N, Baumbach J, Lengauer T, Conklin BR, Albrecht M. AltAnalyze and DomainGraph: analyzing and visualizing exon expression data. Nucleic Acids Res 2010; 38:W755–62.

29. Robinson MD, McCarthy DJ, Smyth GK. edgeR: a Bioconductor package for differential expression analysis of digital gene expression data. Bioinformatics 2010; 26:139–40.

30. McLean CY, Bristor D, Hiller M, Clarke SL, Schaar BT, Lowe CB, Wenger AM, Bejerano G. GREAT improves functional interpretation of cis-regulatory regions. Nat Biotechnol 2010; 28:495–501.

31. Wang J, Duncan D, Shi Z, Zhang B. WEB-based GEne SeT AnaLysis Toolkit (WebGestalt):

update 2013. Nucleic Acids Res 2013; 41:W77–83.

32. Xu J, Kelly R, Fang H, Tong W. ArrayTrack: a free FDA bioinformatics tool to support emerging biomedical research--an update. Hum Genomics 2010; 4:428–34.

33. Horvath S. DNA methylation age of human tissues and cell types. Genome Biol 2013; 14:R115.

34. Delgado-Calle J, Sañudo C, Sánchez-Verde L, García-Renedo RJ, Arozamena J, Riancho JA. Epigenetic regulation of alkaline phosphatase in human cells of the osteoblastic lineage. Bone 2011; 49:830–8.

FIGURE LEGENDS

Fig 1. Methylation analysis of hMSCs. (*A*) Volcano plots of DNA methylation differences in enhancer regions of hMSCs obtained from fractures and OA. Coloured in green, plots with a FDR<0.05 and absolute beta differences larger than 0.1 (*B*) Heat-map showing beta values of enhancer regions. In red more methylated and in green less methylated. Samples are named with a lab identifier code (JAR).

Fig 2. Relationship between methylation and gene expression signatures. (*A*) Venn diagram summarizing the association between differential DNA methylation and differential gene expression (comparisons of hMSCs from fractures over hMSCs from controls). (*B*) Pathways enrichment analysis of genes with hypomethylated enhancers that were up-regulated in fractures.

Fig 3. Epigenetic aging of hMSCs. Left: Comparison of epigenetic and chronological age. Regression lines for each patient group are shown. Right: Deviation from the overall regression line with the two groups combined (mean and SE residuals in each patient group).

Fig 4. Proliferation capacity and expression of selected genes by hMSCs from patients with fractures (FRX) and osteoarthritis (OA). (*A*) Proliferation assessed by Ki67 staining. (*B*) Proliferation by a MTT assay. (*C*) Expression of osteogenic markers by hMSCs from FRX and OA. (*D*) Expression of adipogenic markers by hMSCs.

Fig 5. Differentiation capacity of hMSCs**.** (A) Osteogenic and adipogenic differentiation of hMSCs, as revealed by Alizarin red staining and Oil red staining, respectively. (*B*) Osteogenic differentiation of hMSCs from patients with fractures (FRX) and with osteoarthritis (OA), semiquantitative analysis. (*C*) Alkaline phosphatase activity in hMSC maintained in osteogenic medium. (*D*) Expression of the

osteoblastic differentiation drivers OSX and RUNX2 in hMSCs from patients with FRX and OA maintained in osteogenic medium.

Figure 1

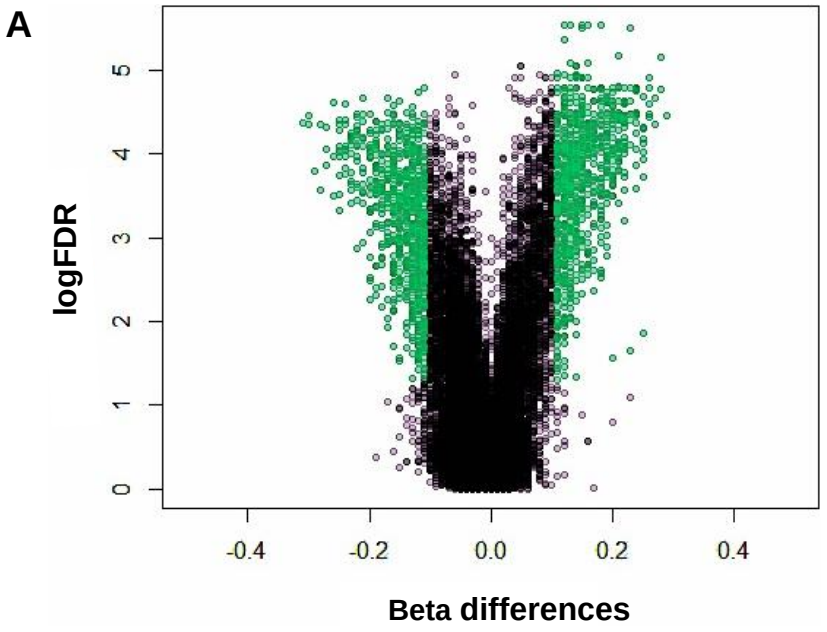
A
logFDR
0
1
2
3
4
5
-0.4
-0.2
0.0
0.2
0.4
Beta differences

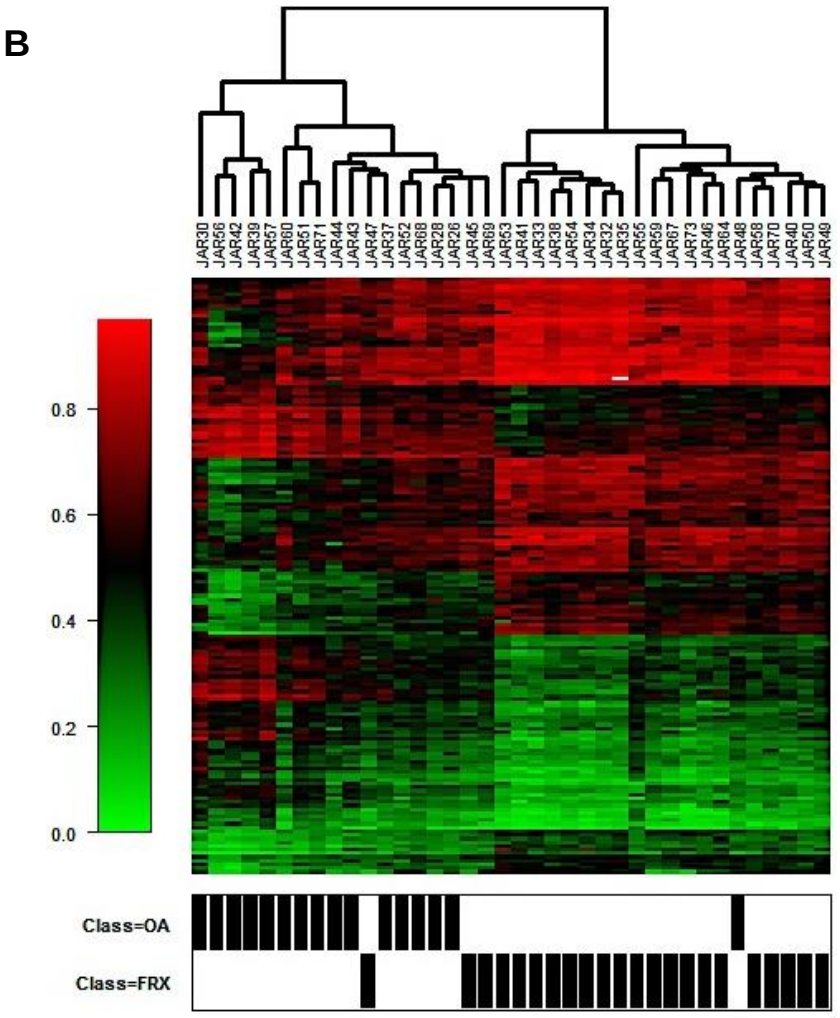
B
JAR30
JAR56
JAR42
JAR39
JAR57
JAR60
JAR51
JAR71
JAR44
JAR43
JAR47
JAR37
JAR52
JAR68
JAR28
JAR26
JAR45
JAR69
JAR53
JAR41
JAR33
JAR38
JAR54
JAR34
JAR32
JAR35
JAR55
JAR59
JAR67
JAR73
JAR46
JAR64
JAR48
JAR58
JAR70
JAR40
JAR50
JAR49
0.0
0.2
0.4
0.6
0.8
Class=OA
Class=FRX

Figure 2

A

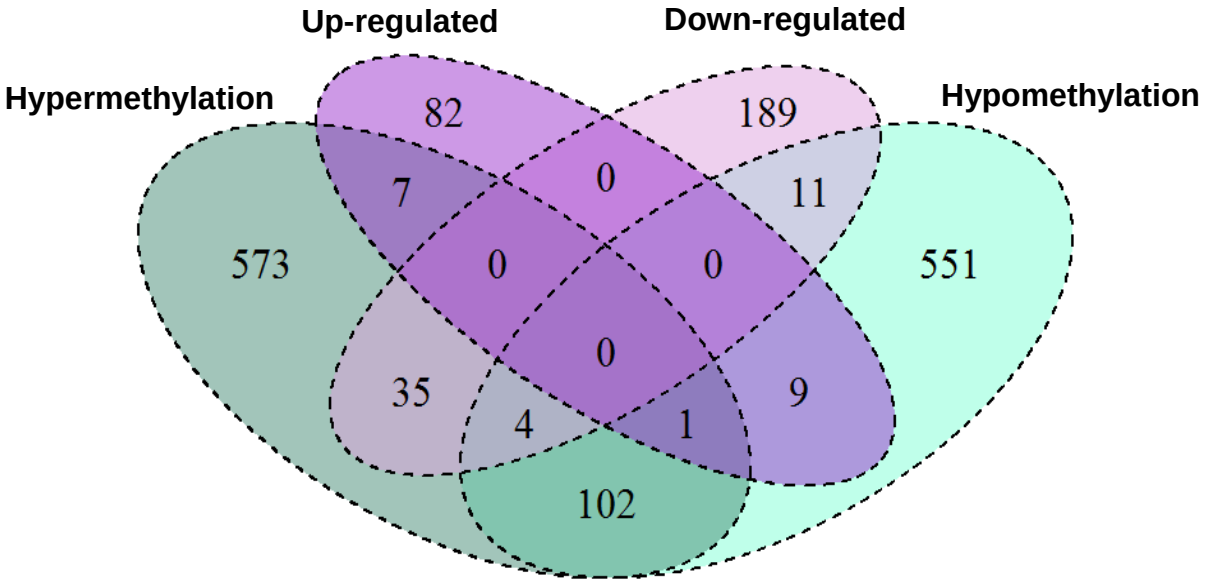
Up-regulated
Down-regulated
Hypermethylation
Hypomethylation
82
189
7
0
11
573
0
0
551
0
35
9
4
1
102

B

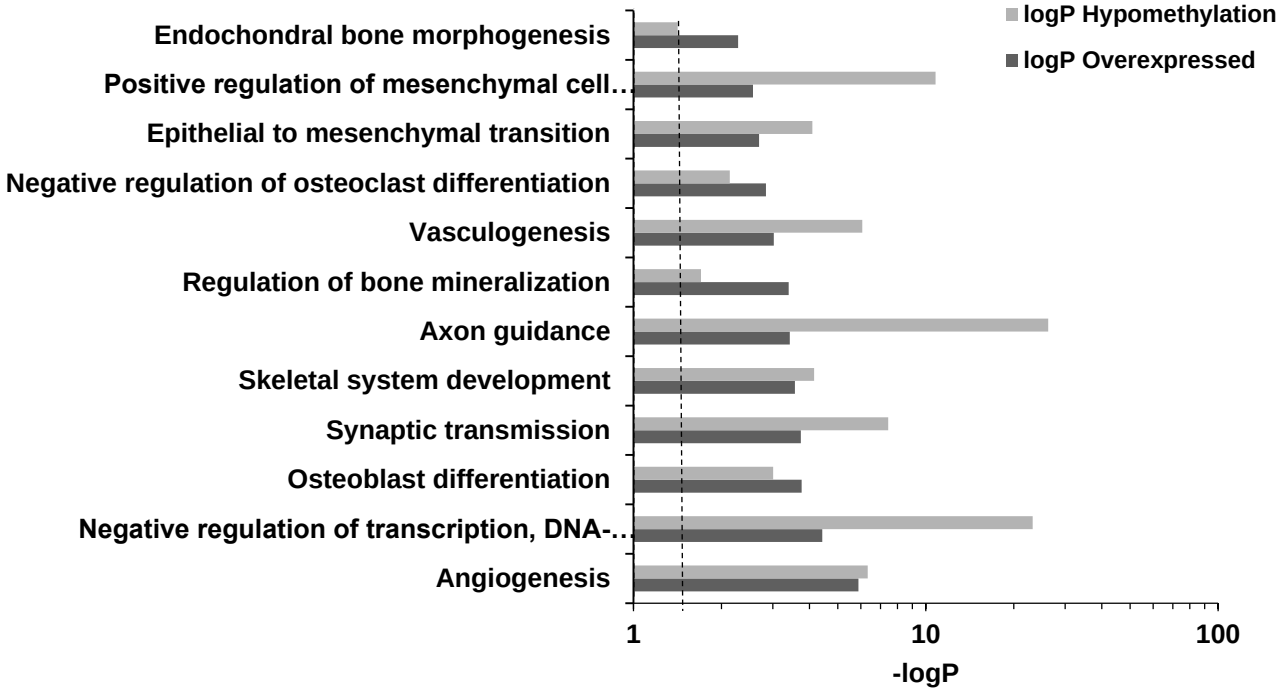
logP Hypomethylation
logP Overexpressed
Endochondral bone morphogenesis
Positive regulation of mesenchymal cell...
Epithelial to mesenchymal transition
Negative regulation of osteoclast differentiation
Vasculogenesis
Regulation of bone mineralization
Axon guidance
Skeletal system development
Synaptic transmission
Osteoblast differentiation
Negative regulation of transcription, DNA-...
Angiogenesis
1
10
100
-logP

Figure 3

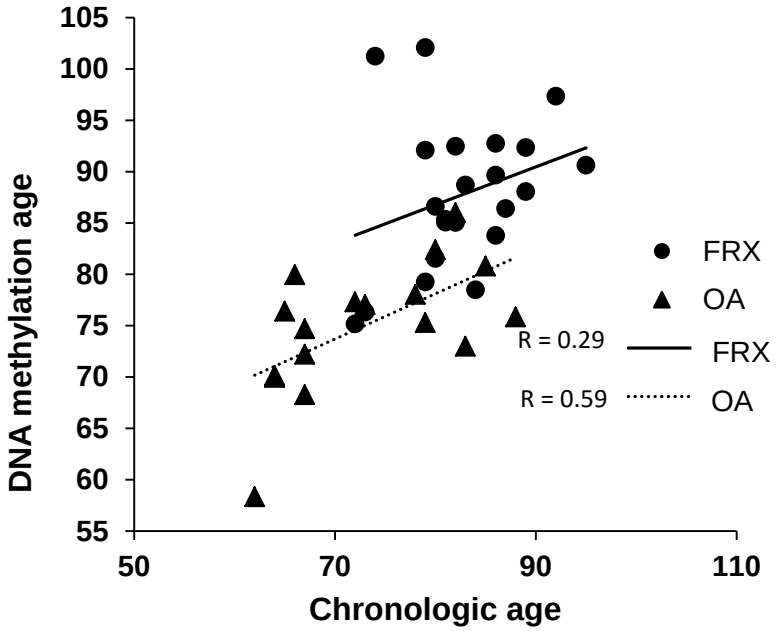
105
100
95
90
85
80
75
70
65
60
55
DNA methylation age
50
70
90
110
Chronologic age
FRX
OA
R = 0.29
FRX
R = 0.59
OA

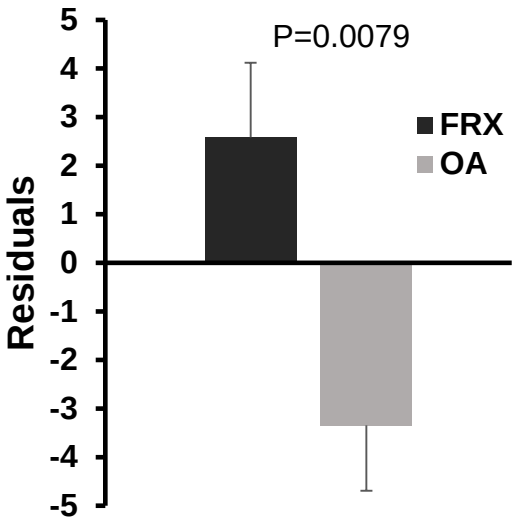
P=0.0079
5
4
3
2
1
0
-1
-2
-3
-4
-5
Residuals
FRX
OA

Figure 4

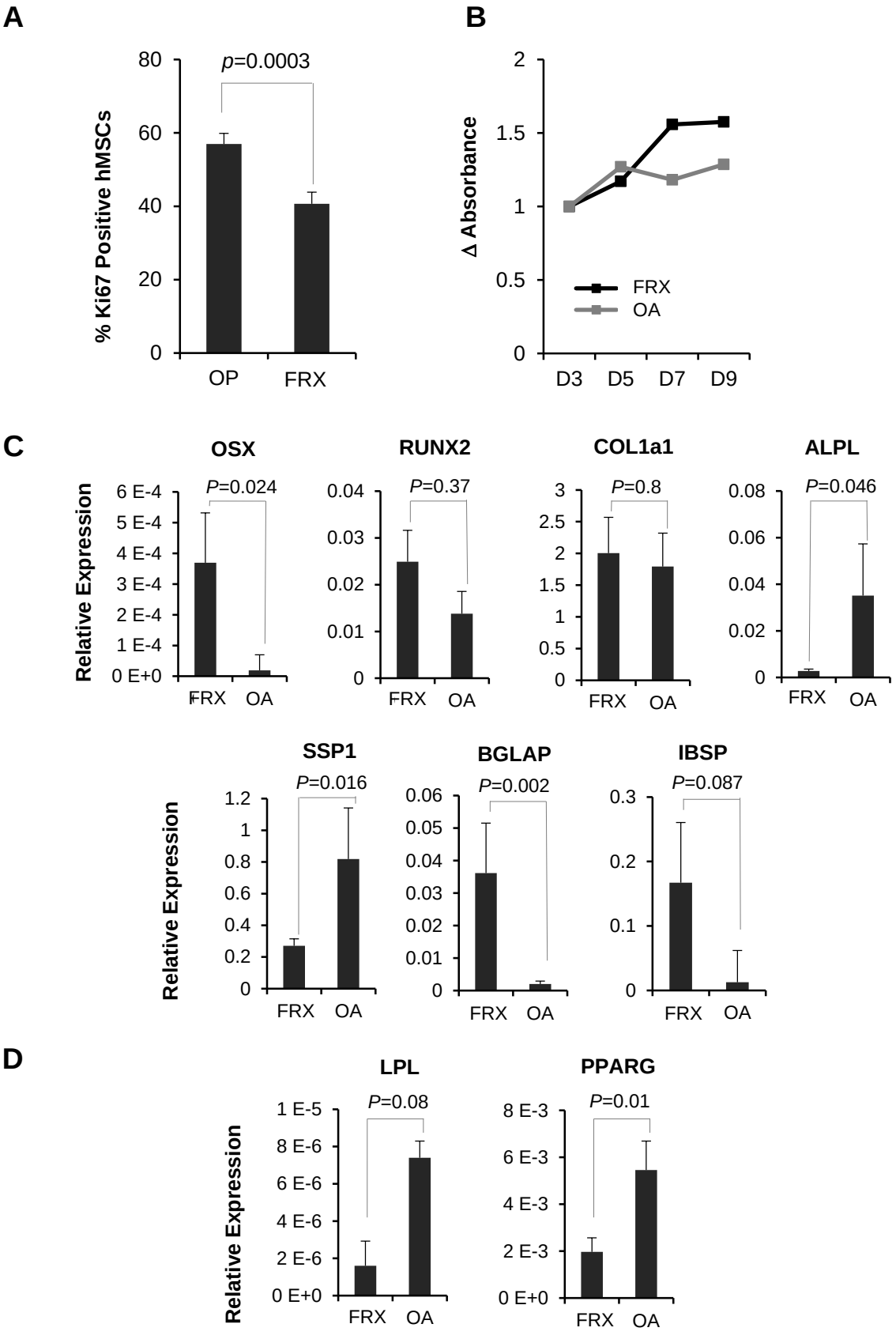
A
p=0.0003
% Ki67 Positive hMSCs
80
60
40
20
0
OP
FRX
B
Δ Absorbance
2
1.5
1
0.5
0
FRX
OA
D3
D5
D7
D9
C
OSX
P=0.024
RUNX2
P=0.37
COL1a1
P=0.8
ALPL
P=0.046
Relative Expression
6 E-4
5 E-4
4 E-4
3 E-4
2 E-4
1 E-4
0 E+0
0.04
0.03
0.02
0.01
0
3
2.5
2
1.5
1
0.5
0
0.08
0.06
0.04
0.02
0
FRX
OA
SSP1
P=0.016
BGLAP
P=0.002
IBSP
P=0.087
1.2
1
0.8
0.6
0.4
0.2
0
0.06
0.05
0.04
0.03
0.02
0.01
0
0.3
0.2
0.1
0
D
LPL
P=0.08
PPARG
P=0.01
1 E-5
8 E-6
6 E-6
4 E-6
2 E-6
0 E+0
8 E-3
6 E-3
4 E-3
2 E-3
0 E+0

Figure 5

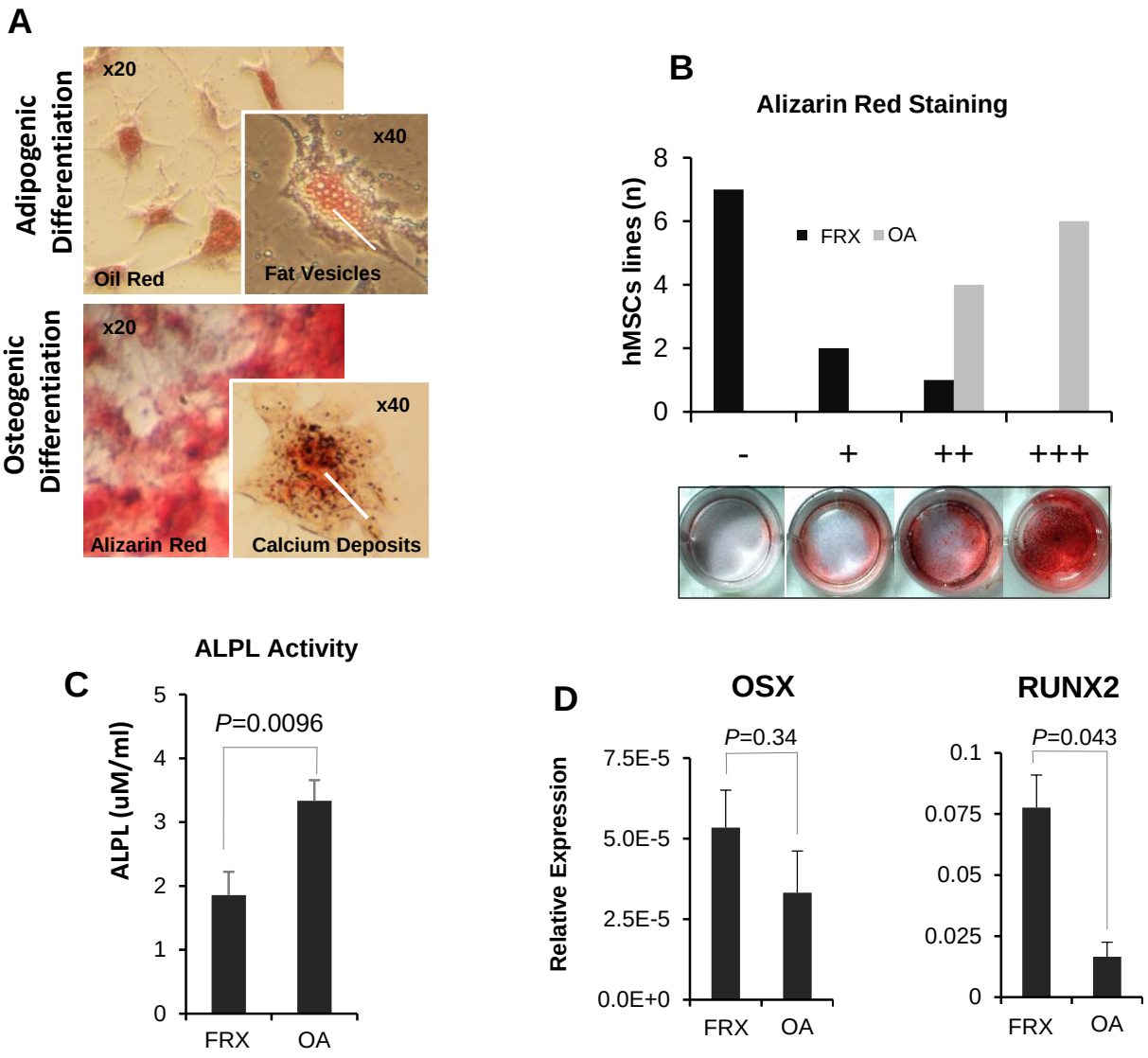
A
Adipogenic Differentiation
x20
x40
Oil Red
Fat Vesicles
Osteogenic Differentiation
x20
x40
Alizarin Red
Calcium Deposits
B
Alizarin Red Staining
hMSCs lines (n)
8
6
4
2
0
FRX
OA
-
+
++
+++
C
ALPL Activity
ALPL (uM/ml)
5
4
3
2
1
0
P=0.0096
FRX
OA
D
OSX
P=0.34
Relative Expression
7.5E-5
5.0E-5
2.5E-5
0.0E+0
FRX
OA
RUNX2
P=0.043
0.1
0.075
0.05
0.025
0
FRX
OA

Table 1. Distribution of differentially methylated CpGs between MSCs from fracture patients (FRX) and patients with osteoarthritis in various genomic regions.

Genomic regions	Differentially methylated CpG sites	Analyzed regions	Differential methylated regions	Regions more methylated in FRX	Regions less methylated in FRX
Promoters	402	30877	217	111	106
Gene bodies	1355	30725	129	62	67
CpG islands	124	26649	40	16	24
Enhancers	2425	41280	1684	870	814

Table 2. Top 50 up-regulated expressed genes in fractures. Gene symbol and complete gene name are shown. Each gene with their corresponding fold change value and corrected p-value (FDR).

Gene symbol	Gene name	Fold-Change	FDR
LGR6	Leucine-Rich Repeat-Containing G-Protein Coupled Receptor 6	11.6	0.0083
BGLAP	Bone Gamma-Carboxyglutamate Protein	10.3	0.0226
GNGT1	G Protein Subunit Gamma Transducin 1	9.1	0.0574
KLRC2	Killer Cell Lectin Like Receptor C2	8.9	0.0083
GLB1L3	Galactosidase Beta 1 Like 3	8.1	0.0046
RANBP3L	RAN Binding Protein 3 Like	7.4	0.0604
PKD1P6	Polycystin 1, Transient Receptor Potential Channel Interacting Pseudogene 6	7.3	0.0163
IBSP	Integrin Binding Sialoprotein	6.1	0.0028
RTEL1	Regulator Of Telomere Elongation Helicase 1	5.8	0.0399
INSC	Inscuteable Spindle Orientation Adaptor Protein	5.7	0.0284
SORCS2	Sortilin Related VPS10 Domain Containing Receptor 2	5.7	0.0383
ACAD8	Acyl-CoA Dehydrogenase Family Member 8	5.0	0.0143
SLC12A7	Solute Carrier Family 12 Member 7	5.0	0.0386
OSBP2	Oxysterol Binding Protein 2	5.0	0.0824
SCN9A	Sodium Voltage-Gated Channel Alpha Subunit 9	4.9	0.0399
BMP2	Bone morphogenetic protein 2	4.8	0.051
LSP1P2	Lymphocyte-Specific Protein 1 Pseudogene 2	4.8	0.0456
ETV1	ETS Variant 1	4.8	0.0979
DNM1	Dynamin 1	4.7	0.0642
TRIM59	Tripartite Motif Containing 59	4.6	0.0815
COL8A2	Collagen type VIII alpha 2 chain	4.1	0.0284
TNNC1	Troponin C1, Slow Skeletal And Cardiac Type	4.1	0.0703
STMN3	Stathmin 3	4.1	0.0274
GRIA1	Glutamate Ionotropic Receptor AMPA Type Subunit 1	4.1	0.0806
LRRC17	Leucine Rich Repeat Containing 17	4.0	0.0854
CACNA1G	Calcium voltage-gated channel subunit alpha1 G	3.9	0.0972
TRIM7	Tripartite Motif Containing 7	3.9	0.0384
ARFRP1	ADP Ribosylation Factor Related Protein 1	3.9	0.095
BTBD11	BTB Domain Containing 11	3.9	0.0924
AMOT	Angiomotin	3.8	0.0129
GALNTL1	Polypeptide N-Acetylgalactosaminyltransferase 16	3.7	0.0686
TNFRSF11B	Osteoprotegerin	3.7	0.0284
NCAM1	Neural Cell Adhesion Molecule 1	3.7	0.0151
RNF112	Ring Finger Protein 112	3.7	0.0797
GALNT3	Polypeptide N-Acetylgalactosaminyltransferase 3	3.6	0.0289
STXBP6	Syntaxin Binding Protein 6	3.6	0.058
ABCA3	ATP Binding Cassette Subfamily A Member 3	3.6	0.0284
MEOX2	Mesenchyme Homeobox 2	3.6	0.0797
TCEAL7	Transcription Elongation Factor A Like 7	3.5	0.0972
EMBP1	Embigin Pseudogene 1	3.5	0.0686

LOXL4	Lysyl Oxidase Like 4	3.5	0.0979
PCDH10	Protocadherin 10	3.5	0.0284
FBXL13	F-Box And Leucine Rich Repeat Protein 13	3.4	0.0183
SYT12	Synaptotagmin 12	3.3	0.0686
LRRC15	Leucine Rich Repeat Containing 15	3.3	0.0884
DNAJC22	DnaJ Heat Shock Protein Family (Hsp40) Member C22	3.1	0.0586
P2RX6	Purinergic Receptor P2X 6	3.1	0.051
CXorf57	Chromosome X Open Reading Frame 57	3.1	0.0284
ENPP1	Ectonucleotide Pyrophosphatase/Phosphodiesterase 1	2.9	0.028
SERPINF1	Serpin Family F Member 1	2.9	0.0609

Table 3. Top 50 down-regulated expressed genes in fractures. Gene symbol and complete gene name are shown. Each gene with their corresponding fold change value and corrected p-value (FDR).

Gene Symbol	Gene name	Fold-Change	FDR
IGHG4	Immunoglobulin Heavy Constant Gamma 4 (G4m Marker)	125.4	0.0274
IGHD	Immunoglobulin Heavy Constant Delta	56.9	0.0279
IGHJ4	Immunoglobulin Heavy Joining 4	48.5	0.0624
IGKV2-28	Immunoglobulin Kappa Variable 2-28	43.4	0.0596
IGHGP	Immunoglobulin Heavy Constant Gamma P	43.1	0.0284
IGKV3-20	Immunoglobulin Kappa Variable 3-20	32.9	0.0183
IGKV4-1	Immunoglobulin Kappa Variable 4-1	26.5	0.0806
IGHG3	Immunoglobulin Heavy Constant Gamma 3	25.1	0.0128
CHL1	Cell Adhesion Molecule L1 Like	22.6	0.0224
SYNPO2	Synaptopodin 2	21.7	0.0018
IGKV1-5	Immunoglobulin Kappa Variable 1-5	21.7	0.0518
IGKV1-6	Immunoglobulin Kappa Variable 1-6	21.7	0.0624
IGLC2	Immunoglobulin Lambda Constant 2	21.6	0.0992
LYZ	Lysozyme	18.1	0.0016
IGHA1	Immunoglobulin Heavy Constant Alpha 1	17.0	0.0199
CHRDL1	Chordin Like 1	16.0	0.0372
CPA3	Carboxypeptidase A3	15.6	0.0651
SLC24A3	Solute Carrier Family 24 Member 3	15.2	0.0182
IGLC3	Immunoglobulin Lambda Constant 3	14.8	0.0967
IGJ	Joining Chain Of Multimeric IgA And IgM	14.2	0.0227
IGHG1	Immunoglobulin Heavy Constant Gamma 1	13.8	0.0339
DERL3	Derlin 3	13.0	0.0486
TMEM176A	Transmembrane Protein 176A	12.8	0.0935
IGLJ3	Immunoglobulin Lambda Joining 3	12.6	0.0856
ACTG2	Actin, Gamma 2, Smooth Muscle, Enteric	12.1	0.0711
IL32	Interleukin 32	11.9	0.0474
CD27-AS1	CD27 Antisense RNA 1	11.6	0.0076
CRISPLD2	Cysteine Rich Secretory Protein LCCL Domain Containing 2	11.3	0.0286
ID4	Inhibitor Of DNA Binding 4, HLH Protein	11.3	0.0028
LPAL2	Lipoprotein(A) Like 2	11.1	0.0058
IGHG2	Immunoglobulin Heavy Constant Gamma 2	10.7	0.038
CP	Ceruloplasmin	10.6	0.0301
NDE1	NudE Neurodevelopment Protein 1	10.4	0.0577
TMTC3	Transmembrane And Tetratricopeptide Repeat Containing 3	10.4	0.0576
SLC5A3	Solute Carrier Family 5 Member 3	9.7	0.0687
STX12	Syntaxin 12	9.6	0.085
HIST1H2AC	Histone Cluster 1 H2A Family Member C	9.6	0.0989
ATXN1L	Ataxin 1 Like	9.6	0.0429
MUC15	Mucin 15, Cell Surface Associated	9.5	0.0204
CHL1-AS2	CHL1 Antisense RNA 2	9.3	0.0207
IGKV3D-20	Immunoglobulin Kappa Variable 3D-20	9.3	0.0824
ARHGAP20	Rho GTPase Activating Protein 20	9.2	0.0337
ADCY2	Adenylate Cyclase 2	9.1	0.0348

SLC22A3	Solute Carrier Family 22 Member 3	8.6	0.0274
PMP22	Peripheral Myelin Protein 22	8.3	0.0358
CDKN1C	Cyclin Dependent Kinase Inhibitor 1C	8.3	0.037
CD38	CD38 Molecule	8.2	0.0972
ENTPD1	Ectonucleoside Triphosphate Diphosphohydrolase 1	8.1	0.0158
TFRC	Transferrin Receptor	7.9	0.0483
KREMEN1	Kringle Containing Transmembrane Protein 1	7.8	0.0769